DNA Strand Arrangement within the SfiI−DNA Complex: Atomic Force Microscopy Analysis†

Alexander Y. Lushnikov,‡ Vladimir N. Potaman,§ Elena A. Oussatcheva,§ Richard R. Sinden,§ and Yuri L. Lyubchenko*,‡

Department of Pharmaceutical Sciences, College of Pharmacy, University of Nebraska Medical Center, 986025 Nebraska Medical Center, Omaha, Nebraska 68198-6025, and Institute of Biosciences and Technology, Texas A&M University Health Sciences Center, 2121 West Holcombe Boulevard, Houston, Texas 77030

Received September 1, 2005; Revised Manuscript Received November 10, 2005

ABSTRACT: The SfiI restriction enzyme binds to DNA as a tetramer holding two usually distant DNA recognition sites together before cleavage of the four DNA strands. To elucidate structural properties of the SfiI−DNA complex, atomic force microscopy (AFM) imaging of the complexes under noncleaving conditions (Ca^{2+} instead of Mg^{2+} in the reaction buffer) was performed. Intramolecular complexes formed by protein interaction between two binding sites in one DNA molecule (cis interaction) as well as complexes formed by the interaction of two sites in different molecules (trans interaction) were analyzed. Complexes were identified unambiguously by the presence of a tall spherical blob at the DNA intersections. To characterize the path of DNA within the complex, the angles between the DNA helices in the proximity of the complex were systematically analyzed. All the data show clear-cut bimodal distributions centered around peak values corresponding to 60° and 120°. To unambiguously distinguish between the crossed and bent models for the DNA orientation within the complex, DNA molecules with different arm lengths flanking the SfiI binding site were designed. The analysis of the AFM images for complexes of this type led to the conclusion that the DNA recognition sites within the complex are crossed. The angles of 60° or 120° between the DNA helices correspond to a complex in which one of the helices is flipped with respect to the orientation of the other. Complexes formed by five different recognition sequences (5′-GGCCNNNNNGGCC-3′), with different central base pairs, were also analyzed. Our results showed that complexes containing the two possible orientations of the helices were formed almost equally. This suggests no preferential orientation of the DNA cognate site within the complex, suggesting that the central part of the DNA binding site does not form strong sequence specific contacts with the protein.

Restriction enzyme SfiI belongs to a family of type II restriction endonucleases that bind simultaneously and cut two cognate sites (type IIf, e.g., ref *1* and references therein). A few type IIf enzymes have been analyzed (Bse634I, Cfr10I, NgoMIV, NaeI, and SfiI), and some details of their mechanisms of action have been revealed. SfiI has been studied extensively by Halford and co-workers [a recent paper (*2*) and references therein]. Crystallographic data have been obtained for Bse634I (*3*), NgoMIV (*4*), and Cfr10I (*5*). SfiI binds as a homotetramer to two recognition sites on DNA duplexes at the recognition sequence 5′-GGCCNNNN∧NGG-CC-3′ (N denotes any base and ∧ marks a cleavage position) prior to cleavage (*6*). The recognition regions can be in one DNA molecule or in two different molecules (cis and trans binding modes). The reaction rate is greater for the cis mode because of the higher effective local concentration of the interacting sites for the intramolecular than for the intermolecular situation (*1*, *6*). Looped DNA structures are formed when the recognition sites are in cis; the protein can efficiently cut sites separated by as few as 104 bp (*7*, *8*) with substantially higher affinity for supercoiled DNA substrates in the case of short distances between the regions. However, there are no data on the SfiI−DNA complex structure, so the organization of the two DNA regions within the protein−DNA complex is not known. Although the sequences at the ends of the recognition region are palindromic, the middle region need not be symmetric. Therefore, the questions of whether the regions are oriented in a particular way, or whether a DNA orientation preference exists within the binding regions of the protein tetramer, also remain unanswered. These questions are addressed in this paper.

We applied atomic force microscopy (AFM)[1] to directly observe SfiI−DNA complexes under noncleaving reaction conditions (Ca^{2+} instead of Mg^{2+} in the reaction buffer). The protein forms synaptic cis or trans type complexes with very high specificity. A systematic analysis of the AFM data showed that DNA recognition sites are crossed at an angle

† This research was supported by Grant GM 062235 (Y.L.L.) from the National Institutes of Health.

* To whom correspondence should be addressed: Department of Pharmaceutical Sciences, College of Pharmacy, University of Nebraska Medical Center, 986025 Nebraska Medical Center, Omaha, NE 68198-6025. Phone: (402) 559-1971. Fax: (402) 559-9543. E-mail: ylyubchenko@unmc.edu.

‡ University of Nebraska Medical Center.

§ Texas A&M University Health Sciences Center.

[1] Abbreviations: AFM, atomic force microscopy; APS, 1-(3-aminopropyl)silatrane.

10.1021/bi051767c CCC: $33.50
Published on Web 12/13/2005

of 60° and the two different relative orientations of the recognition sites are equally populated in the SfiI−DNA complexes.

EXPERIMENTAL PROCEDURES

Materials. Restriction enzymes SfiI, NspI, and HindIII are from New England Biolabs (Beverly, MA). The concentration of SfiI was determined by densitometric scanning of SDS−PAGE gels stained with Coomassie Blue after the electrophoretic runs of commercial SfiI against known quantities of bovine serum albumin (*9*).

DNA Design and Manipulations. Plasmids pEO200, pEOF353, and pEOF504 are derivatives of the pUC8 plasmid with two SfiI recognition sites introduced by site-directed mutagenesis. Briefly, to introduce the first SfiI site, the entire pUC8 was PCR amplified with two overlapping outward-directed primers containing the SfiI sequence. After SfiI digestion, the linear plasmid with the SfiI sticky ends was circularized with T4 DNA ligase. The new plasmid, with one SfiI site, was PCR amplified with two other overlapping primers containing a SfiI sequence, in which the five central base pairs were selected to match the XhoI sequence. After XhoI digestion, the linear plasmid that had the XhoI sticky ends adjacent to the two SfiI half-sites was circularized. Sequences of the SfiI recognition sites (underlined) are listed: plasmid pEO200 (sites **S1**, 5′-TTGGCCACCCCGGCCTT-3′, and **S2**, 5′-TCGGCCTCGAGGGCCTC-3′, are separated by 200 bp), plasmid pEOF353 (sites **S3**, 5′-GTGGCCTTGTGGGCCGA-3′, and **S4**, 5′-GGGGCCTCGAGGGCCAT-3′, are separated by 353 bp), and plasmid pEOF504 (sites **S5**, 5′-CCGGCCGCGTTGGCCGA-3′, and **S4**, 5′-GGGGCCTCGAGGGCCAT-3′, are separated by 504 bp).

Linear DNA fragments with two SfiI sites were obtained by digestion of the plasmid with NspI endonuclease as recommended by the supplier. Double digestion of the plasmid with NspI and HindIII releases two DNA fragments with one SfiI recognition site per fragment. Reactions were carried out as follows: 3−4 μg of plasmid in 50 μL of NEBuffer2 (provided by the supplier) first was incubated with 10 units of HindIII for 1 h at room temperature, and then 5 units of NspI was admixed in the reaction volume, followed by the second incubation for 1 h at 37 °C. Restriction fragments were purified from a 1.8% agarose gel using the QIAquick gel extraction kit (Qiagen Inc., Valencia, CA), ethanol precipitated, and diluted in HE buffer [10 mM HEPES and 1 mM EDTA (pH 7.5)]. The DNA concentration was determined by absorption at 260 nm using the NanoDrop spectrophotometer (NanoDrop Technologies, Wilmington, DE). The complete set of DNA fragments studied in this work is shown in Figure 1.

Preparation of SfiI−DNA Complexes. A typical reaction mixture contained a 1:1 ratio of the protein tetramer per recognition site: 60 fmol of SfiI tetramer and 60 fmol of DNA fragment (with one recognition site) in 10 μL of reaction buffer A [10 mM HEPES (pH 7.5), 50 mM NaCl, 2 mM $CaCl_2$, 0.1 mM EDTA, and 1 mM DTT]. The mixture was incubated for 15 min at room temperature followed by mixing with 10 μL of 0.5% glutaraldehyde [1:1 ratio (v/v)] to cross-link the complex. After cross-linking was carried out for 5 min, the reaction was terminated by adding 1 μL of 2 M Tris-HCl, and the complex was purified by filtration through a UFC7 Millipore column. The filtrate was collected in 20 μL of reaction buffer, and 2−3 μL was deposited onto APS mica.

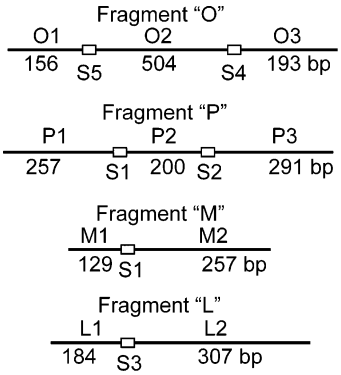

FIGURE 1: Design of DNA fragments used in this paper. The SfiI recognition sites are indicated with open rectangles. The arm−site and intersite distances are given in base pairs. DNA fragments are obtained from plasmids pEO200, pEOF353, and pEOF504 which are derivatives of the pUC8 plasmid with SfiI recognition sites introduced by site-directed mutagenesis.

Atomic Force Microscopy. Procedures for mica modification with 1-(3-aminopropyl)silatrane (APS-mica), the sample preparation, and imaging have been described previously (*10*). Briefly, APS-mica was prepared by treatment of freshly cleaved mica with a 167 μM water solution of APS. DNA samples (3−5 μL) were placed onto APS-mica for 2 min; then the sample was rinsed with deionized water (Labconco Co., Kansas City, MO) and dried with argon. Images were acquired in air using a MultiMode SPM NanoScope IV system (Veeco/Digital Instruments, Santa Barbara, CA) operating in tapping mode. Tapping Mode Etched Silicon Probes (TESP; Veeco/Digital Instruments, Inc.) with a spring constant of ~42 N/m and a resonant frequency of ~320 kHz were used. Image processing and the cross-section, contour length, and angle measurements were performed using Femtoscan (Advanced Technologies Center, Moscow, Russia).

Data Analysis. The size of the protein in the complex was obtained from the volume data (*11*). The complex was approximated by a hemisphere with a diameter measured at half-maximal height of the protein measured from the cross-section analysis (*12*). Streptavidin−DNA complexes were used for the conversion of the volume data into the protein size using the volume value for the streptavidin tetramer (60 kDa) bound to a biotin-labeled DNA (*13*, *14*).

Angles between DNA duplexes at the crossovers decorated with protein particles were measured using the following procedure. A 10 nm long DNA segment (an almost straight section of a DNA filament) just outside the complex was used for the angle measurements (*15*). A line was drawn over the middle of the DNA filament, and the angle between corresponding lines was measured as shown in Figure 2d. The mean values, the standard error of the mean, and the number of measured molecules are given in the histograms and tables.

RESULTS AND DISCUSSION

DNA Design. DNA fragments used in this paper (Figure 1) were obtained by cutting out a selected DNA section from

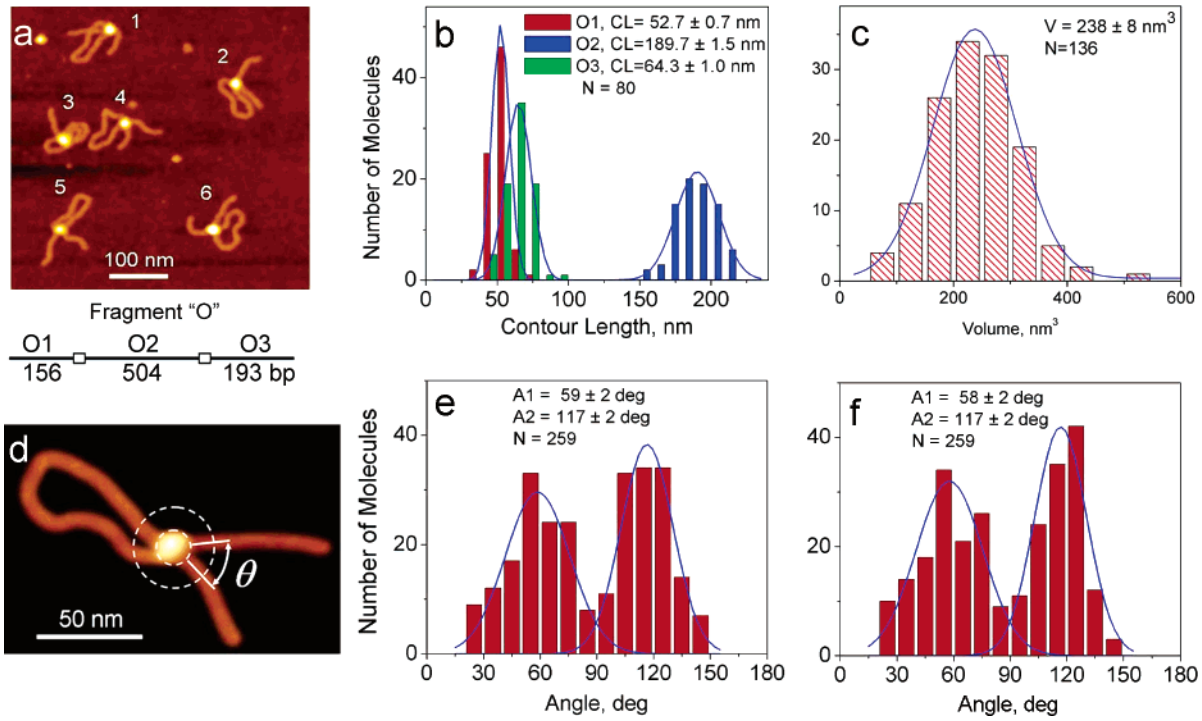

FIGURE 2: AFM images and results of AFM analysis for the SfiI complex in cis with fragment O. (a) AFM image of the 500 nm × 500 nm area with six molecules in the field. A model of the DNA fragment is shown below the image. All molecules on the image have a loop. (b) Histograms of contour length (short arm O1, red; long arm O3, green; and a circumference of the loop O2, blue). (c) Histogram of SfiI volume measurements. The height and diameter at a half-maximal height were obtained from cross-section analysis, and the protein shape was approximated by a hemisphere to calculate the volume (*12*). To convert the SfiI volume data into protein size, the streptavidin−DNA complex was used as a standard with the volume value for the streptavidin tetramer (60 kDa) bound to a biotin-labeled DNA (*13*, *14*). (d) Scheme illustrating the procedure for measurement of the angle Θ between DNA strands in which 10 nm long DNA segments (an almost straight section of DNA) just outside the complex were used for angle measurements (*15*). (e) Histogram of the angles between DNA arms outside the loop. (f) Histogram of the angles between DNA strands inside the loop.

various plasmids. Fragments O and P contained two recognition sites per fragment with 504 and 200 bp between the sites, respectively, and fragments M and L containined one recognition site per fragment. The distances between the ends of the molecules and the closest protein binding site (termed arms) and the distances between two recognition regions (in base pairs) are indicated for each fragment.

AFM Analysis of cis-SfiI−DNA Complexes. The SfiI complexes were obtained in reaction buffer containing 2 mM $CaCl_2$ instead of $MgCl_2$ to prevent DNA cleavage (*16*). SfiI complexes with fragment O are shown in Figure 2a. All DNA molecules on this image have clear-cut looped morphology with a bright spot at the crossover. The looped DNA structures were the predominant morphologies for this type of complex, and they comprised 85% of the DNA molecules that were observed. Other morphologies observed were naked DNA (12%), a complex of protein bound to one recognition site on the DNA fragment (~2%), and a trans type complex with SfiI bound to two DNA fragments (~1%). For the looped structures, the data for measurements of the arm length and the circumferences of the loop are given in Figure 2b. The measured arm lengths were 52.7 ± 0.7 and 64.3 ± 1.0 nm, and the loop size was 189.7 ± 1.5 nm (N = 80). These numbers are in a good agreement with expected values 53, 66, and 171 nm, respectively, calculated from the sequence data using parameters for B-DNA (0.34 nm per base pair), suggesting that specific synaptic complexes formed with high efficiency.

To estimate the size of SfiI in the complex with DNA, we measured the volumes of the protein particles for a large number of synaptic type complexes. The histogram for the volume measurements (Figure 2c) provides a mean value of 238 ± 8 nm^3 (N = 136). We used our AFM data obtained for the streptavidin tetramer (60 kDa) bound to biotinylated sites on DNA (*13*) to convert the SfiI volume into molecular mass. Using the streptavidin tetramer volume (122 nm^3), the calculated molecular mass of SfiI in complex with DNA is 117 kDa, which is very close to the expected mass of a protein tetramer (124 kDa) (*6*, *17*). This finding suggests that the tetramer organization of the protein remains unchanged upon preparation of the sample for AFM.

Table 1: Data for Angles between DNA Strands in the Cis Type of SfiI−DNA Complex[a]

complex type	angle between arms (deg)	angle inside the loop (deg)	no. of complexes analyzed (N)
O, cis	59 ± 2 (49%)	58 ± 2 (48%)	259
	117 ± 2 (51%)	117 ± 2 (52%)	
P, cis	65 ± 3 (44%)	64 ± 2 (57%)	61
	125 ± 4 (56%)	116 ± 1 (43%)	

[a] Relative occurrences of conformations with acute or obtuse angles between specific DNA helices for each construct are given in parentheses.

Images of the molecules in Figure 2a show that the angle between the same DNA helices varied. For example, molecules 4 and 5 have an acute angle between DNA arms, whereas a similar angle for molecules 2 and 6 is obtuse, suggesting that the DNA helices can be oriented differently within the complex. DNA segments adjacent to the protein 10 nm in length (these are normally almost straight sections

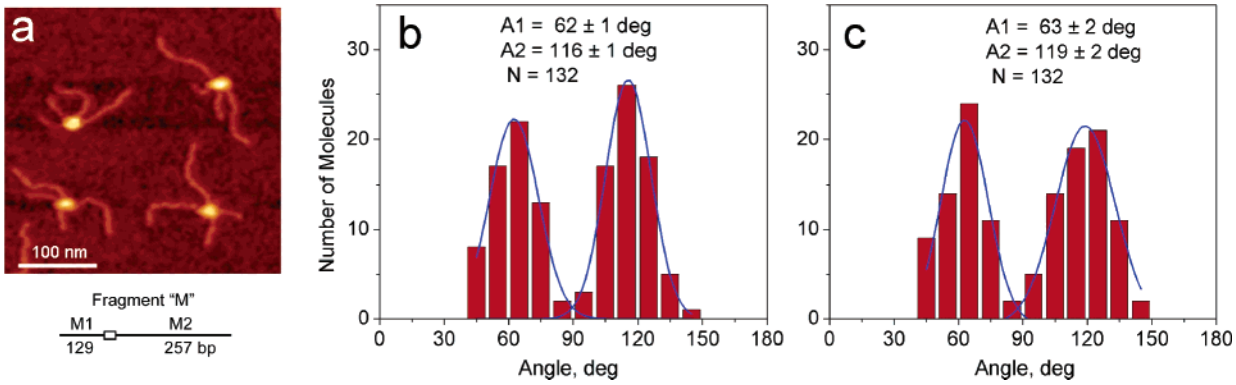

FIGURE 3: SfiI complex with fragment M. AFM image (a) and histograms for the angle between short arms (b) and long arms (c). The model of the DNA fragment is shown under the image.

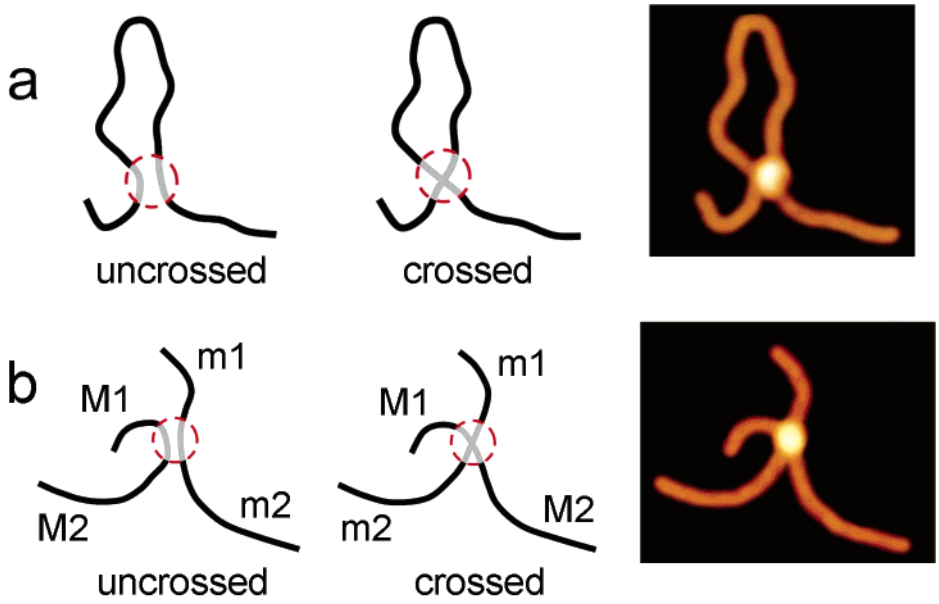

FIGURE 4: Models of the possible arrangements of DNA strands in the synaptic SfiI−DNA complex. (a) Models for the cis type complex with the uncrossed (left) and crossed (center) orientations of the strands. (b) Models for the arrangement of two M fragments within a synaptic complex for uncrossed (left) and crossed DNA strands (center).

of a DNA filament) were used for angle measurements (see schematics in Figure 2d). The data for the angles inside and outside the loops are given in panels e and f of Figure 2, respectively. Both data sets show a bimodal angle distribution with mean values in subpopulations of 59 ± 2° and 117 ± 2° for the angles inside the loop and 58 ± 2° and 117 ± 2° for angles between DNA arms outside the loop. The numbers of molecules with acute and obtuse angle values measured inside and outside of the loop are quite similar (49 and 48% for the acute angle vs 51 and 52% for the obtuse angle, respectively).

Similar analysis was performed for fragment "P" with a 200 bp distance between the recognition sites. The values of the angles within the loop and between the arms were 64 ± 2° (57%) and 116 ± 1° (43%) for the intraloop and 65 ± 3° (44%) and 125 ± 5° (56%) for the interarm measurements, respectively. These angles are very close to those obtained for the larger loop design, as are the population distributions of the two conformational states. The data for angle measurements with the cis type of the complex are summarized in Table 1. These data suggest that two distinct relative orientations for DNA strands within the SfiI tetramer are possible. Importantly, the orientations with an acute angle (ca. 60°) and an obtuse angle (ca. 120°) between DNA helices are relatively equally represented.

AFM Analysis of trans-SfiI−DNA Complexes. In addition to cis complexes, we analyzed the geometry of DNA within trans complexes which are formed by two DNA fragments with one recognition region per fragment. The image of SfiI complexes formed by fragment M is shown in Figure 3a. Trans type complexes of SfiI with two DNA molecules comprised 99% of the complexes that were observed. The SfiI−DNA complexes containing only one DNA fragment were very rare (<1%). The complexes have a symmetric structure with a protein bound to a specific position approximately one-third from one end of the DNA fragment. As for observations for cis type complexes, we found that the angles between the short and long arms varied. Two molecules in the image (Figure 3a) have acute angles, whereas two other have obtuse angles between similar-length DNA arms. The results of the angle measurements for short and long arms are shown as histograms in panels b and c of Figure 3, respectively. As for the cis type SfiI−DNA complexes, a clear bimodal distribution centered around ~60° and ~120° was observed. The populations of molecules with acute and obtuse angles were almost equal. They

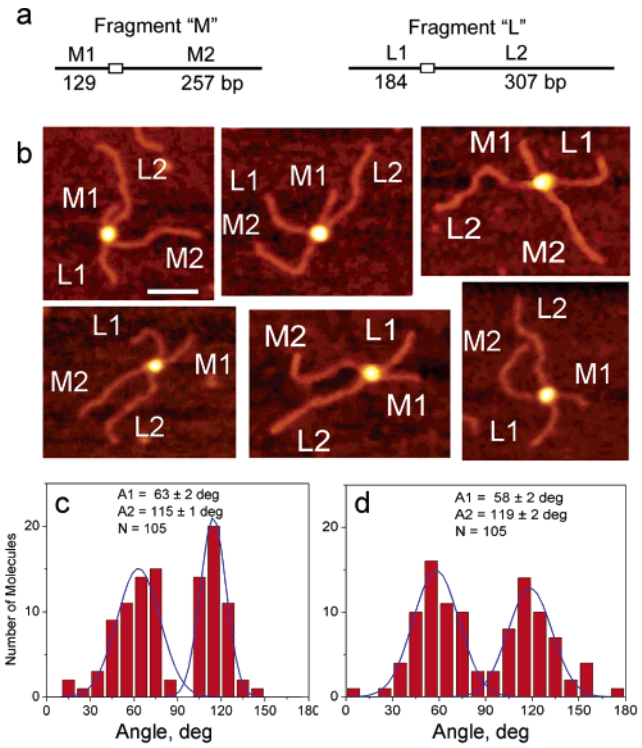

FIGURE 5: (a) Models of DNA fragments. (b) Selected AFM images of the ML type complex assembled by SfiI with two different DNA fragments (M and L). Arms M1 and M2, and L1 and L2, are assigned according to their length measurements. (c and d) Histograms of the angles between the short arms M1 and L1 and the long arms M2 and L2, respectively.

were 47 and 53% for the angle between the short DNA arms and 45 and 55% for the angle between the long arms, respectively.

Model of the Synaptic Complex. Although the data obtained clearly indicate the existence of two types of SfiI−DNA synaptic complexes, they cannot distinguish between two different models for the DNA path in the complex. In one model for the cis complex, shown schematically in Figure 4a (left), DNA is severely bent, whereas an alternative model (Figure 4a, center), in which the DNA helices cross each other, does not require such a bend. The same ambiguity arises for the MM trans type complex as shown in Figure 4b. The path inside the synaptic complex of DNA helices for identical molecules (indicated as M and m**)** cannot be determined unambiguously by AFM. Indeed, as for the schematics for the cis complex, the left model in Figure 4b corresponds to the arrangement of uncrossed DNA helices with an M1−m1−m2−M2 pattern of arm arrangement (clockwise), and the M1−m1−M2−m2 arrangement (Figure 4b, center) corresponds to the model with crossed helices.. Note that the lengths of the DNA helices beyond the protein contour (shown as a circle) are identical in the two models and that AFM images, as shown at the right, cannot distinguish between them.

To resolve this problem and ascertain which of the two models is correct, we analyzed synaptic complexes formed by two fragments with significantly different lengths (386 bp, fragment M, and 491 bp, fragment L; see Figure 5a). The use of two different DNA substrates should result in a mixture of synaptic homocomplexes (MM and LL) and a heterocomplex (ML). We used contour length measurements

Table 2: Data for Angles between DNA Strands in the Trans Type of SfiI−DNA Complex[a]

complex type	angle between short arms (deg)	angle between long arms (deg)	no. of molecules analyzed (*N*)
MM, trans	62 ± 1 (47%)	63 ± 2 (45%)	132
	116 ± 1 (53%)	119 ± 2 (55%)	
LL, trans	64 ± 1 (67%)	61 ± 3 (56%)	83
	130 ± 1 (33%)	127 ± 3 (44%)	
ML, trans	63 ± 2 (54%)	58 ± 2 (53%)	105
	115 ± 1 (46%)	119 ± 2 (47%)	

[a] Relative occurrences of conformations with acute or obtuse angles for each construct are given in parentheses.

to distinguish between these. Images of heterocomplexes (ML) are shown in Figure 5b. Like the data described in the previous sections, these images reveal two classes of protein−DNA complexes: complexes with an obtuse angle between the short DNA arms (L1 and M1) (top row) and those with an acute angle between the short arms (bottom row). The statistics for the angle measurements between the short and long arms in the heterodimer ML are given in Figure 5c,d. As for the cis complex, the distribution is bimodal with mean values of 63 ± 2° and 115 ± 1° for the angle between the shorts arms and 58 ± 2° and 119 ± 2° for the angle between the long arms ($N = 105$). The fractions of molecules with the acute or obtuse angles are approximately equal. This observation is also fully consistent with the results shown above. The angle measurements were performed for homocomplexes LL and MM as well. A complete set of data for the angle measurements in all trans complexes is given in Table 2. In summary, these measurements are consistent with the bimodal distribution for the interarm angles and relatively equal distribution of both types of complexes.

Importantly, the data for DNA fragments with different lengths and different positions of the recognition site in trans (ML heterocomplex) allow us to distinguish between the crossed or bent models. Indeed, each arm of the ML heterodimers was identified by length measurements. The images in Figure 5b show molecules with an unambiguous alternating order of arms of different lengths (mixed orientation), e.g., M1−L2−M2−L1 for molecule 1 and M1−L1−M2−L2 for molecule 3 in the top row. These data support the crossed orientation model of the DNA helices within the SfiI−DNA complex (Figure 4b, middle), as this pattern would not be expected for the bent model.

We found that 80% of all ML type complexes have this alternating pattern of arm orientation. Another 20% of molecules represent equally two types of complexes, M1−M2−L1−L2 and M1−M2−L2−L1, that can be assigned to the uncrossed model in Figure 4b. We suggest a possible explanation for the appearance of the two types of AFM images of the heterocomplexes and for the finding that the complex with a crossed orientation of the arms prevails over the alternative orientation. We should take into consideration the three-dimensionality of the synaptic complex formed by a large protein tetramer and consider different projections of the complex on a plane that are good approximations for flat AFM images. Let us, for simplicity, approximate the protein as a cylinder with DNA bound to the top and bottom sides of the cylinder (Figure 6). The DNA helices, according to our data, are crossed at a 60° angle; therefore, we arrange

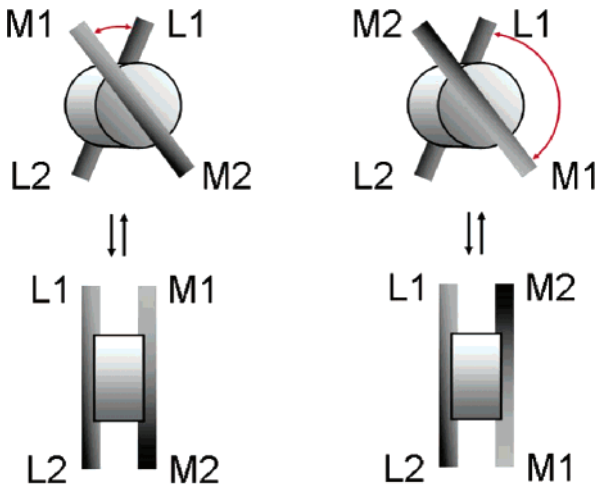

FIGURE 6: Three-dimensional models for SfiI−DNA complexes with DNA fragments M and L. The protein is shown as a thick disk with DNA bound to the both sides of the disk. In the top row, an acute angle between short arms L1 and M1 is shown on the left in which the DNA "binding" planes are parallel to the surface plane. The same orientation of the complex relative to the plane, but with the orientation of the fragment M flipped (top right), exhibits an obtuse angle between arms L1 and M1. The bottom row shows the orientation of the top complexes in a way that the cylinder's planes (the DNA "binding" planes) are perpendicular to the surface plane.

the DNA helices on the top and bottom planes of the cylinder according to the crossed model and consider two relative orientations of the DNA helices, M1−L1−M2−L2 and M1−L2−M2−L1 (Figure 6, top). If this complex approaches the surface with any of its cylinder sides, we will obtain the projections with the alternating orientation of the arms, i.e., M1−L1−M2−L2 and M1−L2−M2−L1. However, if we consider a projection in which the sides of the cylinder are perpendicular to the plane (90° rotation, Figure 6, bottom), the DNA duplexes will be parallel and the arms can adopt the L1−M1−M2−L2 or L1−M2−M1−L2 orientation when the molecule flattens on the plane. Given the relatively high rigidity of the DNA helix, these projections will be less favorable. This prediction is consistent with our results supporting the model with a crossed orientation of the duplex for the SfiI−DNA complex. We cannot exclude the possibility that the DNA helices within the complex are distorted in such a way that they are not straight. This distortion will lead to additional nonplanar geometry in the complex that in turn may facilitate the formation of projections of the arms in an L1−M2−M1−L2 arrangement. In addition, we cannot formally exclude the possibility that drying of the sample during the 2 min following deposition will also increase the yield of complexes in this orientation.

What is the reason for the bimodal distribution of the angle between the arms? Is this due to the existence of two different conformations of the SfiI tetramer? We found that the bimodal character of the angle distribution is a general property of the complex regardless of the type of complex (cis or trans) or the sequence in the center of the recognition region. Therefore, this observation can be explained assuming that recognition of the GGGG- - - - -GGCC inverted repeats within the binding site is important in complex formation. This assumption is supported by the observation that the central part of the entire DNA binding region (5′-GGC-CNNNNNGGCC-3′) is not essential for binding specificity, as the protein very likely has no contacts with the bases inside the spacer (*18*). If two recognition slots on the protein surfaces crossed at a fixed angle 60°, a simple change in the relative orientation of the DNA helices will change the interarm angle from 60° to 120° (Figure 6, top schemes). Therefore, the change in the helix orientation will lead to a bimodal angle distribution as observed experimentally. The protein recognition sequence for SfiI has the dyad symmetry only at the flanks; therefore, our data suggest that the middle part of the DNA binding region (at least for the sequences studied in this work) is not essential for the recognition, and very likely plays primarily the role of a spacer required to keep the GGCC/CCGG flanks at a specific distance.

An interesting prediction from the proposed model for the SfiI−DNA complex can be drawn for the cis type of synaptic complex. The flip between 60° and 120° orientations can also change the shape of DNA loop in cases when the loop size is relatively small and comparable with DNA persistence length. In the case of the acute orientation of the helices, the loop is elongated along one axis. In the alternative orientation with the obtuse angle, the loop is deformed along a perpendicular axis making it wider. The difference in loop shape can affect the mobility of the complex in the gel. Indeed, two types of looped DNA−SfiI complexes with different gel mobilities have been observed (*8*). However, we cannot exclude the possibility that a change in DNA topology can also contribute to the gel mobility of the two conformers as discussed previously (*8*).

Given a homotetramer composition of SfiI within the functional complex with DNA, the finding that the DNA helices are arranged at a 60° rather than orthogonal angle is seemingly counterintuitive. Indeed, the orthogonal orientation of DNA helices was assumed previously (*8*). However, from crystallographic data available for three type IIf restriction enzymes, Bse6341 (*3*), CfrI (*5*), and NgoMIV (*4*), the orientations of the monomer units within the tetramer are far from being orthogonal, suggesting that DNA helices can be arranged in a nonorthogonal orientation as well. Moreover, Deibert et al. (*4*) recently showed that inside the NgoMIV complex the DNA helices are bound to two distant protein binding clefts located at the protein surface with a relative orientation of the helices of ca. 60°. The coincidence of the orientation pattern for this protein and SfiI is remarkable. Although both proteins operate as tetramers, the recognition site for NgoMIV (5′-GCCGGC-3′) is much shorter than that of SfiI. Moreover, unlike NgoMIV that binds to a continuous hexameric site, the recognition site for SfiI contains a 5 bp spacer, the sequence of which is not essential for the recognition, suggesting loose contacts, if any, between the protein moieties and the DNA bases in the middle part of the DNA cognate site. Additional structural studies of these proteins are needed to elucidate the mechanisms of their actions and their mechanistic similarities and differences.

ACKNOWLEDGMENT

We thank M. Karymov, L. Shlyakhtenko, and O. Sankey for stimulating discussion about the data and the critical comments.

REFERENCES

1. Embleton, M. L., Siksnys, V., and Halford, S. E. (2001) DNA cleavage reactions by type II restriction enzymes that require two copies of their recognition sites, *J. Mol. Biol. 311*, 503−514.

2. Embleton, M. L., Vologodskii, A. V., and Halford, S. E. (2004) Dynamics of DNA loop capture by the SfiI restriction endonuclease on supercoiled and relaxed DNA, *J. Mol. Biol. 339*, 53−66.
3. Grazulis, S., Deibert, M., Rimseliene, R., Skirgaila, R., Sasnauskas, G., Lagunavicius, A., Repin, V., Urbanke, C., Huber, R., and Siksnys, V. (2002) Crystal structure of the Bse634I restriction endonuclease: Comparison of two enzymes recognizing the same DNA sequence, *Nucleic Acids Res. 30*, 876−885.
4. Deibert, M., Grazulis, S., Sasnauskas, G., Siksnys, V., and Huber, R. (2000) Structure of the tetrameric restriction endonuclease NgoMIV in complex with cleaved DNA, *Nat. Struct. Biol. 7*, 792−799.
5. Siksnys, V., Skirgaila, R., Sasnauskas, G., Urbanke, C., Cherny, D., Grazulis, S., and Huber, R. (1999) The Cfr10I restriction enzyme is functional as a tetramer, *J. Mol. Biol. 291*, 1105−1118.
6. Wentzell, L. M., Nobbs, T. J., and Halford, S. E. (1995) The SfiI restriction endonuclease makes a four-strand DNA break at two copies of its recognition sequence, *J. Mol. Biol. 248*, 581−595.
7. Wentzell, L. M., and Halford, S. E. (1998) DNA looping by the Sfi I restriction endonuclease, *J. Mol. Biol. 281*, 433−444.
8. Watson, M. A., Gowers, D. M., and Halford, S. E. (2000) Alternative geometries of DNA looping: An analysis using the SfiI endonuclease, *J. Mol. Biol. 298*, 461−475.
9. Van Komen, S., Petukhova, G., Sigurdsson, S., and Sung, P. (2002) Functional cross-talk among Rad51, Rad54, and replication protein A in heteroduplex DNA joint formation, *J. Biol. Chem. 277*, 43578−43587.
10. Shlyakhtenko, L. S., Gall, A. A., Filonov, A., Cerovac, Z., Lushnikov, A., and Lyubchenko, Y. L. (2003) Silatrane-based surface chemistry for immobilization of DNA, protein-DNA complexes and other biological materials, *Ultramicroscopy 97*, 279−287.
11. Ratcliff, G. C., and Erie, D. A. (2001) A novel single-molecule study to determine protein−protein association constants, *J. Am. Chem. Soc. 123*, 5632−5635.
12. Henderson, R. M., Schneider, S., Li, Q., Hornby, D., White, S. J., and Oberleithner, H. (1996) Imaging ROMK1 inwardly rectifying ATP-sensitive K^+ channel protein using atomic force microscopy, *Proc. Natl. Acad. Sci. U.S.A. 93*, 8756−8760.
13. Lushnikov, A. Y., Brown, B. A., II, Oussatcheva, E. A., Potaman, V. N., Sinden, R. R., and Lyubchenko, Y. L. (2004) Interaction of the Zα domain of human ADAR1 with a negatively supercoiled plasmid visualized by atomic force microscopy, *Nucleic Acids Res. 32*, 4704−4712.
14. Potaman, V. N., Lushnikov, A. Y., Sinden, R. R., and Lyubchenko, Y. L. (2002) Site-specific labeling of supercoiled DNA at the A+T rich sequences, *Biochemistry 41*, 13198−13206.
15. Pavlicek, J. W., Oussatcheva, E. A., Sinden, R. R., Potaman, V. N., Sankey, O. F., and Lyubchenko, Y. L. (2004) Supercoiling-induced DNA bending, *Biochemistry 43*, 10664−10668.
16. Milsom, S. E., Halford, S. E., Embleton, M. L., and Szczelkun, M. D. (2001) Analysis of DNA looping interactions by type II restriction enzymes that require two copies of their recognition sites, *J. Mol. Biol. 311*, 515−527.
17. Nobbs, T. J., Szczelkun, M. D., Wentzell, L. M., and Halford, S. E. (1998) DNA excision by the Sfi I restriction endonuclease, *J. Mol. Biol. 281*, 419−432.
18. Williams, S. A., and Halford, S. E. (2001) SfiI endonuclease activity is strongly influenced by the non-specific sequence in the middle of its recognition site, *Nucleic Acids Res. 29*, 1476−1483.

BI051767C